A Photonic RF Phase Shifter Based on a Dual-Parallel Mach–Zehnder Modulator and an Optical Filter

Applied Physics Express **5** (2012) 072502
http://dx.doi.org/**10.1143/APEX.5.072502**

A Photonic RF Phase Shifter Based on a Dual-Parallel Mach–Zehnder Modulator and an Optical Filter

Jianguo Shen[1,2], Guiling Wu[1]*, Weiwen Zou[1], and Jianping Chen[1]

[1]*State Key Laboratory of Advanced Optical Communication Systems and Networks, Shanghai Key Laboratory of Navigation and Location Based Services, Department of Electronic Engineering, Shanghai Jiao Tong University, Shanghai 200240, China*
[2]*College of Mathematics, Physics and Information Engineering, Zhejiang Normal University, Jinhua 321004, China*

Received May 8, 2012; accepted June 18, 2012; published online July 5, 2012

A photonic RF phase shifter using a dual parallel Mach–Zehnder modulator (DPMZM) and a tunable optical band-pass filter is demonstrated. The dependences of the linearity and power stability of the proposed RF phase shifter on the performance of the DPMZM and the optical filter are theoretically analyzed and numerically simulated. In the experiment, a continuously tunable range of more than 450° phase shift and a small power variation of less than 1.6 dB for a wideband RF range (8–12 GHz) are achieved by simply tuning the bias voltage of the DPMZM. The experimental results agree well with the theoretical analysis. © 2012 The Japan Society of Applied Physics

Due to the advantages of broad bandwidth, light weight, and immunity to electromagnetic interferences, photonic radio frequency (RF) shifters are expected to play important roles in phased-arrayed beam-forming and microwave photonic filters.[1–3] To date, various schemes for photonic RF phase shifters have been proposed,[4–9] and most of them include two separate modules of RF modulation and phase shift process. The phase shift process was implemented using a complicated module based on different approaches such as optical fiber true delay network,[4] stimulated Brillouin scattering (SBS) effect in optical fibers,[5–7] slow and fast light effect in semiconductor optical amplifier (SOA).[8,9] Such a configuration of two complicated modules makes the system costly and inconvenient for practical applications.

Recently, an *x*-cut dual-parallel Mach–Zehnder modulator (DPMZM) was used to generate carrier phase-shifted double sideband (CPS-DSB) modulation and the phase difference between the optical carrier and the two sidebands can be tuned by changing the bias voltage of the DPMZM.[10] Usually, there is no RF phase shift according to the principle of the vector sum because the two RF signals produced by beating between the optical carrier and the two individual sidebands have the same amplitude but inverse phase. However, it is possible to phase-shift the RF signal by introducing asymmetry between the two sidebands. In ref. 12, the SBS effect was utilized to deplete one of the two sidebands and amplify the other. An additional pump and a long-length optical fiber for SBS made the scheme sophisticated and tended to be instable. Optical filtering was proposed to suppress one of the sidebands in measuring the basic delay of the microwave photonic filter in ref. 12. Actually it has not been used to realize a photonic RF phase shifter.

In this paper, we demonstrate a simple and effective photonic RF phase shifter using a DPMZM and a commercial tunable optical band-pass filter (TOBPF). The working principle of the phase shifter is in details studied. Theoretical and numerical analyses are carried out to investigate the effects of the extinction ration (ER) of the DPMZM and the suppression ration (SR) of two sidebands induced by the TOBPF on the linearity and power stability of the phase shifter. A range of more than 450° phase shift with power variation of less than 1.6 dB for a wideband range of 8–12 GHz is experimentally obtained that matches well the theoretical analysis.

*E-mail address: wuguiling@sjtu.edu.cn

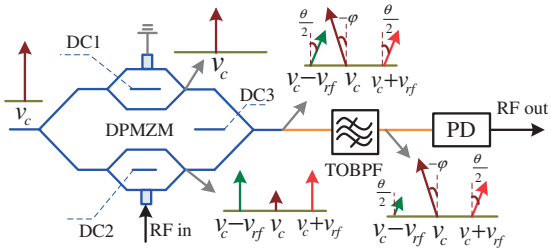

Fig. 1. Schematic of the RF phase shifter based on DPMZM and TOBPF.

Figure 1 shows the schematic of the proposed RF photonic phase shifter. An optical carrier is launched into an *x*-cut DPMZM, which comprises two parallel sub-MZMs lying on two arms of a parent MZM.[12] No RF signal is applied on the sub-MZM on the top arm, which works at the maximum transmission point to ensure optical carrier passing fully. The other sub-MZM on the bottom arm is driven by a RF signal and biased at the null transmission point in order to perform carrier-suppressed double sideband modulation. A CPS-DSB signal can be generated at the output of the DPMZM,[11] which can be expressed by

$$\begin{aligned} E_1(t) = {} & A_1 \exp\left[j\left(2\pi v_c t - \frac{\theta}{2}\right)\right] \\ & + A_2 \exp\left\{ j\left[(2\pi v_c + v_{rf})t + \frac{\theta}{2}\right]\right\} \\ & + A_2 \exp\left\{ j\left[(2\pi v_c - v_{rf})t + \frac{\theta}{2}\right]\right\} \\ & + k_1 A_1 \exp\left[j\left(2\pi v_c t + \frac{\theta}{2}\right)\right], \end{aligned} \tag{1}$$

where A_1 (A_2) is the amplitude of the optical carrier (sidebands) and v_c (v_{rf}) is the frequency of the optical carrier (RF signal). k_1^2 represents the optical carrier power ratio between the bottom arm and the top arm of the parent MZM. When the bias voltage DC1 operates at the maximal point and DC2 at the null point, k_1^{-2} equals the ER of the DPMZM. The phase difference between the carrier and sidebands is expressed by

$$\theta = \pi V_3 / V_{\pi 3}, \tag{2}$$

where V_3 is the bias voltage DC3 of the parent MZM and $V_{\pi 3}$ is its half-wave voltage. By combining the two optical carriers from two arms, eq. (1) can be further simplified to as

$$E_2(t) = A\exp[j(2\pi v_c t - \varphi)] + A_2\exp\left\{j\left[(2\pi v_c + v_{rf})t + \frac{\theta}{2}\right]\right\} + A_2\exp\left\{j\left[(2\pi v_c - v_{rf})t + \frac{\theta}{2}\right]\right\}, \quad (3)$$

where

$$A = A_1[1 + k_1^2 + 2k_1\cos(\theta)]^{1/2}, \quad (4)$$

$$\varphi = \tan^{-1}\left[\frac{\sin(\theta/2) - k_1\sin(\theta/2)}{\cos(\theta/2) + k_1\cos(\theta/2)}\right]. \quad (5)$$

From eqs. (4) and (5), due to the finite ER of the modulator, the power of the optical carrier fluctuates periodically and the phase shift is nonlinear when the bias voltage DC3 is tuned. After passing through the TOBPF, assuming that the lower sideband is partly suppressed, the electric field is given by

$$E_3(t) = A\exp[j(2\pi v_c t - \varphi)] + A_2\exp\left\{j\left[(2\pi v_c + v_{rf})t + \frac{\theta}{2}\right]\right\} + k_2 A_2\exp\left\{j\left[(2\pi v_c - v_{rf})t + \frac{\theta}{2}\right]\right\}, \quad (6)$$

where k_2^{-2} is the suppression ratio (SR) of the optical power between the upper and lower sidebands induced by the TOBPF.

The phase-shifted RF current can be produced by the beating between two individual sidebands and the optical carrier at the photo detector (PD), which can be expressed by

$$i(t) \propto E_3(t) \times E_3^*(t) = B\cos(2\pi v_{rf} t + \phi), \quad (7)$$

where

$$B = 2A_1 A[1 + k_2^2 + 2k_2\cos(\theta + 2\varphi)]^{1/2}, \quad (8)$$

$$\phi = \tan^{-1}\left[\frac{\sin(\theta/2 + \varphi) - k_2\sin(\theta/2 + \varphi)}{\cos(\theta/2 + \varphi) + k_2\cos(\theta/2 + \varphi)}\right]. \quad (9)$$

In eq. (7), we neglect the DC and second harmonic components for simplicity. As can be seen from eq. (9), one can easily control the phase shift by tuning the bias voltage DC3 if k_2 does not equal 1. One can also see that the phase-shift linearity and power stability, i.e., two key features of the phase shifter, are related to the ER of the DPMZM and SR induced by the TOBPF.

It should be noted that the linearity and power stability of the phase shifter in this paper are characterized by the deviation from ideal linearity according to eq. (2) and output power variation, respectively. Figure 2 shows the linearity and power stability as functions of the bias voltage (V_3) under different sets of ER and SR. From it, one can see that the same ER and SR value introduce the same peak-to-peak deviation from linearity and power variation on the phase shifter with different periods. The performance of the phase shifter can be improved by increasing the values of ER and SR. The parameters, such as ER = 21 dB and SR = 44 dB, are set according to the actual situation for comparison convenience with the experimental study.

The experiment setup to verify the theoretical analysis is depicted in Fig. 3. A distributed-feedback (DFB) laser diode provides an optical carrier with an optical power of 12 dBm. A DPMZM (Photline MXIQ-LN-40) is used to generate CPS-DSB modulation with a half-wave voltage

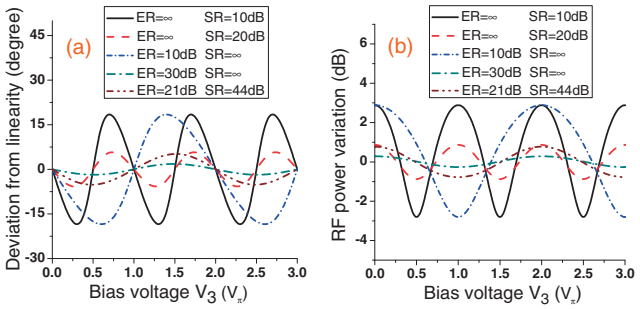

Fig. 2. Numerical analysis of the dependences of RF phase shift deviation from linearity (a) and power variation (b) on the different sets of ER and SR.

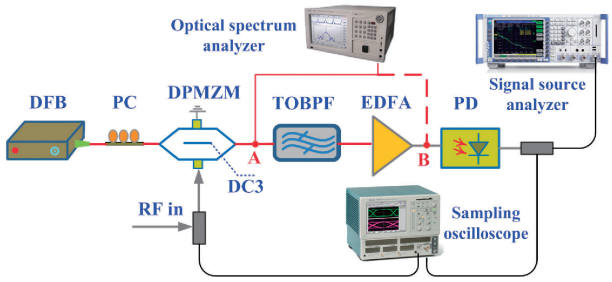

Fig. 3. Experimental setup of the proposed photonic RF phase shifter. DFB, distributed feedback laser; DPMZM, dual-parallel Mach–Zehnder modulator; PC, polarization controller; EDFA, erbium-doped fiber amplifier; TOBPF, tunable optical band-pass filter; PD, photo detector.

(DC3) of about 14 V. One of the sidebands is suppressed by a TOBPF (Alnair BLV-200CL) with tunable bandwidth and central frequency. An erbium-doped fiber amplifier (EDFA) is applied to compensate the insertion loss of the DPMZM and the TOBPF. The RF signal is finally recovered with a 50 GHz PD (u^2t XPDV2150R). A high speed digital sampling oscillator (Tektronix TDS8200) and a signal source analyzer (R&S FSUP) are utilized to measure the phase shift and the power stability of the output RF signal, respectively.

In the experiment, the bias voltage DC1 is tuned at the maximal point (4.8 V) and DC2 is tuned at the null point (9.4 V). The central frequency and bandwidth of TOBPF are adjusted to make the lower sideband signal in the TOBPF's stopping band and the upper sideband signal in the TOBPF's passing band. Figure 4 shows the optical spectrum of the CPS-DSB signal at the output of the DPMZM (a) and EDFA (b) (points "A" and "B" in Fig. 3) measured using a high resolution optical spectrum analyzer (Apex AP2040A) when the input RF signal has the frequency of 10 GHz and the power of 13 dBm. The TOBPF's transmission response is also illustrated in Fig. 4(b). From it, we can see that the lower sideband of the CPS-DSB signal can be efficiently suppressed with an SR of 44 dB.

As shown in the transmission response of the TOBPF [Fig. 4(b)], the proposed RF phase shifter is suitable for wideband application and the bandwidth can be extended by simply changing the bandwidth of the TOBPF. The phase shift, linearity, and power stability versus the bias voltage (V_3) for different RF frequencies of 8, 9, 10, 11, and 12 GHz are measured and shown in Fig. 5. A nearly linear phase shift of more than 450° and a power variation of less than

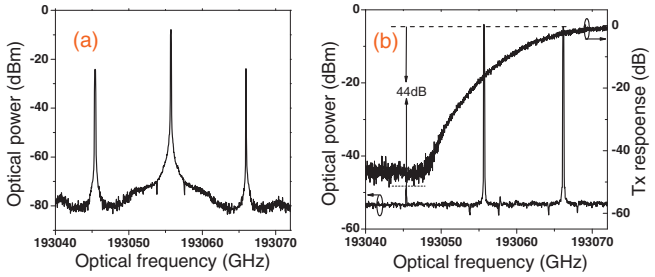

Fig. 4. Measured optical spectrums of (a) CPS-DSB signal launched from the DPMZM, and (b) at the output of the EDFA. In (b), the TOBPF's transmission response is also depicted.

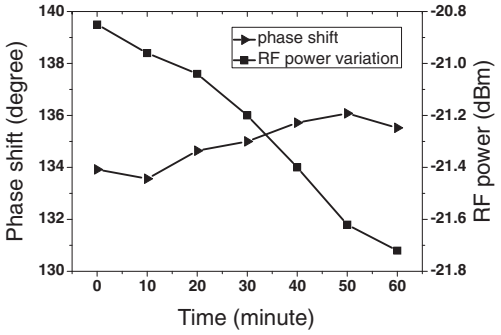

Fig. 6. The stability of the photonic RF phase shifter.

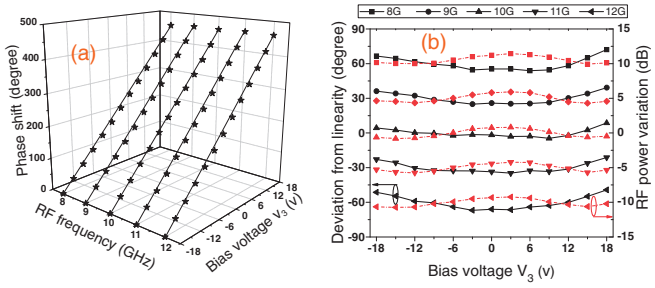

Fig. 5. Measured dependences of RF phase shift (a), deviation from the linearity, and power variation (b) on the bias voltage of DPMZM at 8–12 GHz. In (b), the deviation from the linearity (RF power variations) for 8–12 GHz is intentionally attenuated by 60° (10 dB), 30° (5 dB), 0 (0), −30° (−5 dB), and −60° (−10 dB), respectively.

1.6 dB are achieved within a wide bandwidth (8–12 GHz) when the bias voltage (V_3) is tuned from −18 to 18 V. The range of RF phase shift corresponds to the optical phase shift of about 455°. The slight deviation of less than 8° from the ideal linearity may be attributed to the inherent nonlinear phase response of the parent MZM at the higher bias voltage, except for the finite ER of the DPMZM (21 dB). The RF power variation is mainly due to the finite ER of the DPMZM. The results agree well with the theoretical analysis shown in Fig. 2. The stability of the RF power and phase shift is also studied at 10 GHz (see Fig. 6). In 1-h period, the phase drift is less than 2° and the power variation is less than 1 dB, respectively. The slight instability is mainly attributed to the slight drift of the central frequency of the TOBPF.

In conclusion, a photonic RF phase shifter using a single-drive DPMZM combining with a TOBPF is theoretically analyzed and experimentally demonstrated. A continuous and nearly linear phase shift of more than 450° and a power variation of less than 1.6 dB are achieved within a wide bandwidth range of 8–12 GHz by simply tuning the dc bias voltage of the parent MZM of the DPMZM from −18 to 18 V. The RF bandwidth can be further extended to a range of 8–20 GHz by adjusting the bandwidth of the TOBPF. The maximum frequency is currently limited by the available bandwidth of the DPMZM in our experiment (20 GHz) and the minimum frequency is due to half of the transition band of the optical filter (8 GHz) to ensure that the lower sideband signal is in the TOBPF's stopping band while the upper sideband signal is in the TOBPF's passing band.

Acknowledgments This work was supported in part by the 973 Program (2011CB301700), the National Natural Science Foundation of China (61071011, 61127016, 61007052, and 61107041), the STCSM Project (10DJ1400402), the State Key Lab Project (GKZD030021), the International Cooperation Project from the Ministry of Science and Technology of China (2011FDA11780), and the Zhejiang provincial Nature Science Foundation of China (LY12F05002).

1) S. Tonda-Goldstein, D. Dolfi, A. Monsterleet, S. Formont, J. Chazelas, and J. P. Huignard: IEEE Trans. Microwave Theory Tech. **54** (2006) 847.
2) J. Capmany, B. Ortega, and D. Pastor: J. Lightwave Technol. **24** (2006) 201.
3) Y. Yu and J. P. Yao: IEEE Photonics Technol. Lett. **19** (2007) 1472.
4) X. W. Li, L. M. Peng, S. B. Wang, Y. C. Kim, and J. P. Chen: Opt. Express **15** (2007) 16760.
5) X. Sun, S. Fu, K. Xu, J. Zhou, P. Shum, J. Yin, X. Hong, J. Wu, and J. Lin: IEEE Trans. Microwave Theory Tech. **58** (2010) 3206.
6) D. B. Adams and C. K. Madsen: J. Lightwave Technol. **26** (2008) 2712.
7) A. Loayssa and F. J. Lahoz: IEEE Photonics Technol. Lett. **18** (2006) 208.
8) J. Sancho, J. Lloret, I. Gaslla, S. Sales, and J. Capmany: Opt. Express **19** (2011) 17421.
9) W. Q. Xue, S. Sales, J. Capmany, and J. Mork: Opt. Express **18** (2010) 6156.
10) S. Y. Li, X. P. Zheng, H. Y. Zhang, and B. K. Zhou: Opt. Lett. **36** (2011) 546.
11) W. Li, N. H. Zhu, L. X. Wang, J. S. Wang, J. G. Liu, Y. Liu, X. Q. Qi, L. Xie, W. Chen, X. Wang, and W. Han: Opt. Express **19** (2011) 12312.
12) K. Higuma, S. Oikawa, Y. Hashimoto, H. Nagata, and M. Izutsu: Electron. Lett. **37** (2001) 515.